

Causal bounds for outcome-dependent sampling in observational studies

Erin E. Gabriel^{1*}

Michael C. Sachs¹

Arvid Sjölander^{1*}

¹:Department of Medical Epidemiology and Biostatistics, Karolinska Institutet, Stockholm, Sweden

★The authors contributed equally to this work.

corresponding author: erin.gabriel@ki.se

March 24, 2022

Abstract

Outcome-dependent sampling designs are common in many different scientific fields including ecology, economics, and medicine. As with all observational studies, such designs often suffer from unmeasured confounding, which generally precludes the nonparametric identification of causal effects. Nonparametric bounds can provide a way to narrow the range of possible values for a nonidentifiable causal effect without making additional assumptions. The nonparametric bounds literature has almost exclusively focused on settings with random sampling and applications of the linear programming approach. We derive novel bounds for the causal risk difference in six settings with outcome-dependent sampling and unmeasured confounding. Our derivations of the bounds illustrate two general approaches that can be applied in other settings where the bounding problem cannot be directly stated as a system of linear constraints. We illustrate our derived bounds in a real data example involving the effect of vitamin D concentration on mortality.

Keywords: Case-control studies; Causal inference; Direct acyclic graphs; Nonparametric bounds; Test-negative designs

*EEG is partially supported by Swedish research council grant 2017-01898.

1 Introduction

The aim of empirical research is often to estimate the causal effect of a particular exposure on a particular outcome. In observational (i.e. not randomized) studies, this is typically complicated by the fact that there are confounders (i.e. common causes) of the exposure and the outcome. Often, these confounders are at least partly unmeasured, in which case the causal effect of interest is generally nonidentifiable as any observable association could be due to the uncontrolled common causes.

One way to narrow the possible range of a nonidentifiable causal effect is to derive bounds, i.e. a range of values that are guaranteed to contain the true causal effect given the true distribution of the observed data. [e.g. Robins, 1989, Balke and Pearl, 1997, Zhang and Rubin, 2003, Cai et al., 2008, Sjölander, 2009]. Generally, the width of these bounds depends on the amount of information provided by the study design; the more information the tighter the bounds. In particular, Balke and Pearl [1997] showed that the bounds for the causal risk difference may be substantially improved upon if an instrumental variable (IV) is available. In their work, Balke and Pearl [1994] defined an algorithm for deriving valid and tight bounds when the causal effect of interest and the constraints implied by the causal model (in the sense of Pearl [2009]) can be stated as a linear optimization problem. Much of the subsequent work on bounds has used this algorithm.

The literature on bounds for causal effects has focused on simple random sampling. However, in many studies the probability of selection into the study depends on the outcome of interest. Such outcome-dependent sampling often has advantages over simple random sampling, such as increased statistical power when the outcome is rare, but it also complicates

the analysis and interpretation of results [Didelez et al., 2010]. The case-control design, and its variations, is perhaps the most common outcome-dependent design. Ideally, in this design, the sampling only depends on the outcome, and not on other variables in the study; we refer to this and all similar studies as *uncounfounded outcome-dependent sampling*. However, this ideal is difficult to achieve in reality.

More often, selection will be confounded with the outcome and exposure. A test-negative design is an example of a confounded outcome-dependent sampling design. In a test-negative study, subjects are selected from the group of patients seeking health care for a particular set of symptoms that are indicative of the disease of interest. Subjects are included in the study if they are tested for disease status based on their symptoms, and the exposure of interest is then retrospectively ascertained. This design, and variations of it, have been discussed extensively in the literature [Sullivan et al., 2014, Sullivan and Cowling, 2015, Sullivan et al., 2016]. An important difference between the case-control design and the test-negative design is that, in the latter, potentially unobserved characteristics, such as the subject’s lifestyle or health-seeking behavior, may influence whether the subject is tested and therefore selected into the study. These characteristics may also be confounders for the exposure (e.g. vaccination status) and the outcome of the study; we refer to this and all similar studies as *confounded outcome-dependent sampling*.

In addition to being confounded with the outcome and exposure, sampling may directly depend on the exposure. We refer to this as *confounded exposure- and outcome-dependent sampling*. Although this is a setting that one hopes to avoid when sampling is outcome-dependent, it may arise in test-negative studies when receiving the exposure reduces one’s threshold for seeking medical treatment. This may also be the case in studies where the

exposure is itself a medical condition and having such a condition leads to increased medical monitoring and therefore an increased probability of being included in the study independent of the outcome.

For each of these three sampling scenarios, we consider the bounds when there is and is not an available IV. In the test-negative design, which is a confounded sampling, outcome-, and possibly exposure-dependent setting, a possible IV is randomization of particular health care centers to provide the exposure, for example a vaccine. Individuals at those health care centers would then be free to decide if they wished to use the vaccine, regardless of their randomized encouragement. For the unconfounded outcome-dependent sampling designs, a possible IV may be a genetic allele, as in so-called Mendelian randomization studies [Bowden and Vansteelandt, 2011].

In this paper we derive bounds for the causal risk difference under six versions of outcome-dependent sampling, which cover if not all, most of the plausible outcome-dependent sampling settings. As conditioning on sampling selection, as well as the lack of confounding of the selection variable, do not result in a clearly linear problem, we cannot use the method of Balke and Pearl [1994] without modification; see Balke [1995] for more detail. Therefore, in addition to providing novel bounds in six relevant scenarios, we also provide an approach to derive valid and informative bounds in some nonlinear scenarios and for modifying some seemingly nonlinear settings so that they are linear programming problems, which to our knowledge have not previously been described in the bounds literature. In addition, we numerically compare the bounds derived in each setting to each other and random sampling via simulations and in a real data example. This describes, in terms possibly easier to convey to practitioners, the information loss associated with outcome-dependent sample selection.

The paper is structured as follows. In Section 2 we define the causal target parameter, provide basic definitions, assumptions and pertinent previously derived bounds. In Section 3 we present the bounds for the target parameter, and in Section 4 we carry out a simulation study to assess the performance of the bounds. In Section 5 we provide a real data example, before providing a summary of our results and a discussion of future work in Section 6.

2 Preliminaries

2.1 Notation

Let X and Y be the exposure and outcome of interest, and $Y(x)$ be the potential (or counterfactual) outcome for a given subject, if the exposure were set to level x [Rubin, 1974, Pearl, 2009]. Let Z be a valid and available IV for X and Y ; we refer readers to Glymour et al. [2012] for details on testing for validity of a candidate IV. We assume X , Y and Z are all fully observed and binary. Let S be an indicator of being selected into the study; $S = 1$ for ‘selected’ and $S = 0$ for ‘not selected’. Let U represent the set of unobserved confounders for X and Y , and sometimes S ; there are no restrictions on the distribution of U . Thus, the observed data distribution is given by $p\{Z, X, Y|S = 1\}$, when an IV is available, and by $p\{X, Y|S = 1\}$ when an IV is not available; $p\{\cdot\}$ denotes the probability mass function. Because U is unmeasured, no counterfactual probabilities of the type $p\{Y(x) = y\}$ are identifiable in any of our settings of interest. Our target parameter is the most common estimand used in nonparametric causal bounds, the causal risk difference

$$\theta = p\{Y(x = 1) = 1\} - p\{Y(x = 0) = 1\}.$$

For convenience of notation, we define several probability abbreviations. Let

$$p_{xy} = p\{X = x, Y = y\},$$

$$p_{xy.s} = p\{X = x, Y = y | S = s\},$$

$$p_{xys} = p\{X = x, Y = y, S = s\},$$

$$p_{xy.zs} = p\{X = x, Y = y | Z = z, S = s\},$$

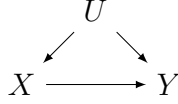
$$p_{xys.z} = p\{X = x, Y = y, S = s | Z = z\},$$

$$r = p\{S = 1\} \text{ and,}$$

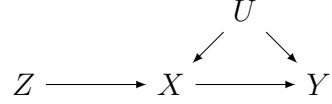
$$r_z = p\{S = 1 | Z = z\}.$$

2.2 Settings

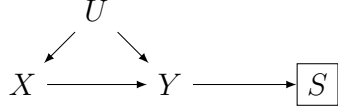
The causal diagrams (as defined by Pearl [2009]) in Figures 1a, 1c, 1e and 1g illustrate random, unconfounded outcome-dependent, confounded outcome-dependent, and confounded exposure- and outcome-dependent sampling, respectively, without an available IV. The causal diagrams in Figures 1b, 1d, 1f and 1h illustrate the corresponding sampling schemes with an available IV. The square around S in Figures 1c, 1d, 1e, 1f, 1g and 1h indicates that the observed data distribution is conditioned on $S = 1$, i.e. on selection into the study. The presence of an arrow from Y to S in the Figures makes the sampling outcome-dependent. The absence of an arrow from U to S in Figures 1c and 1d makes the sampling unconfounded, whereas the presence of this arrow in Figures 1e-1h makes the sampling confounded. In Figures 1b, 1d, 1f and 1h, Z has a causal effect on X . This is stronger than is necessary; in order for Z to be a valid IV it is enough for Z to be associated with X .



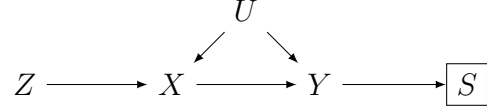
(a) Random sampling, without IV.



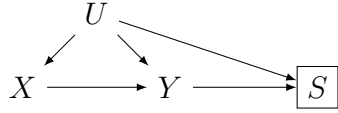
(b) Random sampling, with IV.



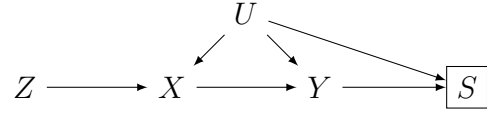
(c) Unconfounded outcome-dependent sampling, without IV.



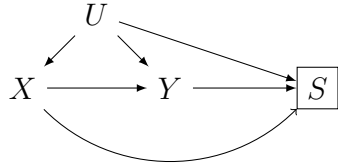
(d) Unconfounded outcome-dependent sampling, with IV.



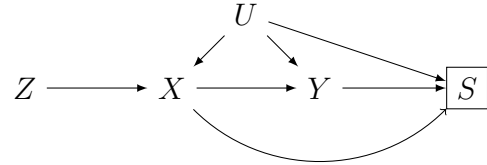
(e) Confounded outcome-dependent sampling, without IV.



(f) Confounded outcome-dependent sampling, with IV.



(g) Confounded exposure- and outcome-dependent sampling, without IV.



(h) Confounded exposure- and outcome-dependent sampling, with IV.

Figure 1: Causal diagrams for eight possible study designs, two of which are random sampling and the other six are outcome-dependent sampling.

2.3 Available information

To provide tight and valid bounds on θ when the sampling is confounded, we find it is necessary to have knowledge of quantities that are not estimable from the observed data distributions, $p\{Z, X, Y|S = 1\}$ or $p\{X, Y|S = 1\}$, alone. In particular, we assume that the sampling prevalence $p\{S = 1\}$ is known. In finite populations, $p\{S = 1\}$ is simply the sample size divided with the population size. For example, in test-negative designs, $p\{S = 1\}$ could be considered the proportion of subjects who were tested for the disease status, among the total number of eligible subjects that were initially included into the study. When one

considers a super-population, $p\{S = 1\}$ could be thought of as the true data generating mechanism of sampling, which remains constant regardless of the infinite population, e.g. flipping a coin for each new case or control that is encountered.

When there is an available IV (Figures 1d, 1f and 1h) we additionally assume that the IV prevalence $p\{Z = 1\}$ is known. When the IV is the randomization of health care centers to provide the vaccine, as may be the case in a test-negative study, $p\{Z = 1\}$, is determined by design. When the IV is a genetic allele, $p\{Z = 1\}$ is often known from previous research. We use the observed data distribution together with $p\{S = 1\}$ and $p\{Z = 1\}$ to calculate $p\{S = 1|Z = z\}$, for $z \in \{0, 1\}$, as $p\{S = 1|Z = z\} = p\{Z = z|S = 1\}p\{S = 1\}/p\{Z = z\}$.

When the sampling is outcome-dependent but unconfounded, X is independent of S given Y (Figures 1c and 1d). Therefore, if $p\{Y\}$ were known, one could recover the unconditional distributions $p\{X, Y\}$ and $p\{Z, X, Y\}$ from the observed conditional data distributions. Thus, previously developed bounds for θ under random sampling could be applied. However, knowing the outcome prevalence is not sufficient to recover the unconditional distributions $p\{X, Y\}$ and $p\{Z, X, Y\}$ when the outcome-dependent sampling is confounded (Figures 1e-1h). Therefore, to allow for equitable comparison of the derived bounds, we consider the same external information in all scenarios, i.e. $p\{S = 1\}$, without an IV and $p\{S = 1\}$ and $p\{Z = 1\}$ with an IV.

2.4 Previous bounds

Robins [1989] derived bounds for θ under random sampling. Without an available IV, the

bounds by Robins [1989] are given by

$$-(p_{01} + p_{10}) \leq \theta \leq 1 - (p_{01} + p_{10}). \quad (1)$$

Robins [1989] also derived bounds in the setting when an IV is available. However, Balke and Pearl [1997] showed that those bounds are valid but not tight, using the linear programming method of bounds derivation developed in Balke [1995] and presented in Balke and Pearl [1994]. Briefly, this method uses the fact that if all of the observed data probabilities can be written as linear combinations of underlying counterfactual probabilities, then maximizing and minimizing the causal risk difference, θ , under the linear constraints defined by these relations is a linear programming problem. **XXXXXX fix this Using fundamental concepts in the field of linear programming, one can prove that the global extrema obtained from the linear programming formulation yield bounds that are tight [Dantzig, 1963]. “Tight” here means that all values inside the bounds are logically compatible with the observed data distribution, under the assumptions (e.g. causal diagram) that were used to derive the bounds.** The bounds derived by [Balke and Pearl, 1997] with an available IV are well known and have been cited numerous times in the causal inference literature [e.g. Greenland, 2000, Frangakis and Rubin, 2002, Hernán and Robins, 2006]; we reproduce these bounds in Equations (1) and (2) of the supplementary material.

3 Novel Bounds

3.1 Unconfounded outcome-dependent sampling

Unconfounded outcome-dependent sampling is illustrated in Figures 1c and 1d, without and with an available IV, respectively. The absence of an arrow from U to S in Figures 1c and 1d makes the derivation of bounds challenging. This is because the absence of this arrow imposes nonlinear constraints, making the linear program method of Balke [1995] not directly applicable. For these settings we define $A(y, s) = p_{1y.s}/p_{0y.s}$ and $B(y, z, s) = p_{1y.zs}/p_{0y.zs}$.

Result 1:

The bounds given in (2) and (3) are valid for θ in the setting of Figure 1c provided that $p_{0y.1} \neq 0 \forall y$, or for $\theta^* = -\theta$ if x is replaced with $x^* = 1 - x$ everywhere in (2) and (3), provided that $p_{1y.1} \neq 0 \forall y$.

$$\theta \geq -(p_{01.1} + p_{10.1})r - \max \left\{ \frac{1}{1 + A(1, 1)}, \frac{A(0, 1)}{1 + A(0, 1)} \right\} (1 - r) \quad (2)$$

and

$$\theta \leq 1 - (p_{01.1} + p_{10.1})r - \min \left\{ \frac{1}{1 + A(1, 1)}, \frac{A(0, 1)}{1 + A(0, 1)} \right\} (1 - r). \quad (3)$$

Result 2:

The bounds given in (4) and (5) are valid for θ in the setting of Figure 1e provided $p_{0y1.z} \neq 0 \forall y, z$, or for $\theta^* = -\theta$ if x is replaced everywhere in (4) and (5) with $x^* = 1 - x$, provided

that $p_{1y1.z} \neq 0 \forall y, z$.

$$\theta \geq \max \left\{ \begin{array}{l} p_{11.11}r_1 + p_{00.01}r_0 - 1 \\ p_{11.01}r_0 + p_{00.11}r_1 - 1 \\ (p_{11.01} - p_{10.01} - p_{01.01})r_0 - (p_{11.11} + p_{01.11})r_1 - \frac{B(0,0,1)}{1+B(0,0,1)}(1-r_0) - (1-r_1) \\ (p_{11.11} - p_{10.11} - p_{01.11})r_1 - (p_{11.01} + p_{01.01})r_0 - \frac{B(0,1,1)}{1+B(0,1,1)}(1-r_1) - (1-r_0) \\ -(p_{10.11} + p_{01.11})r_1 - \max \left\{ \frac{1}{1+B(1,1,1)}, \frac{B(0,1,1)}{1+B(0,1,1)} \right\} (1-r_1) \\ -(p_{10.01} + p_{01.01})r_0 - \max \left\{ \frac{1}{1+B(1,0,1)}, \frac{B(0,0,1)}{1+B(0,0,1)} \right\} (1-r_0) \\ (p_{00.11} - p_{10.11} - p_{01.11})r_1 - (p_{10.01} + p_{00.01})r_0 \\ - \max \left\{ \frac{1}{1+B(1,1,1)}, -\frac{1-B(0,1,1)}{1+B(0,1,1)} \right\} (1-r_1) - (1-r_0) \\ (p_{00.01} - p_{10.01} - p_{01.01})r_0 - (p_{10.11} + p_{00.11})r_1 \\ - \max \left\{ \frac{1}{1+B(1,0,1)}, -\frac{1-B(0,0,1)}{1+B(0,0,1)} \right\} (1-r_0) - (1-r_1) \end{array} \right\}, \quad (4)$$

and

$$\theta \leq \min \left\{ \begin{array}{l} 1 - p_{10.11}r_1 - p_{01.01}r_0 \\ 1 - p_{10.01}r_0 - p_{01.11}r_1 \\ (p_{10.11} + p_{00.11})r_1 + (p_{11.01} + p_{00.01} - p_{10.01})r_0 \\ \quad + (1 - r_1) + \max \left\{ \frac{1-B(0,0,1)}{1+B(0,0,1)}, \frac{B(1,0,1)}{1+B(1,0,1)} \right\} r_0 \\ (p_{11.11} + p_{00.11} - p_{10.11})r_1 + (p_{10.01} + p_{00.01})r_0 \\ \quad + \max \left\{ \frac{1-B(0,1,1)}{1+B(0,1,1)}, \frac{B(1,1,1)}{B(1,1,1)} \right\} (1 - r_1) + (1 - r_0) \\ (p_{11.11} + p_{00.11})r_1 + \max \left\{ \frac{1}{1+B(0,1,1)}, \frac{B(1,1,1)}{1+B(1,1,1)} \right\} (1 - r_1) \\ (p_{11.01} + p_{00.01})r_0 + \max \left\{ \frac{1}{1+B(0,0,1)}, \frac{B(1,0,1)}{1+B(1,0,1)} \right\} (1 - r_0) \\ (p_{11.11} + p_{00.11} - p_{01.11})r_1 + (p_{11.01} + p_{01.01})r_0 \\ \quad + \max \left\{ \frac{1}{B(0,1,1)}, -\frac{1-B(1,1,1)}{1+B(1,1,1)} \right\} (1 - r_1) + (1 - r_0) \\ (p_{11.01} + p_{00.01} - p_{01.01})r_0 + (p_{11.11} + p_{01.11})r_1 \\ \quad + \max \left\{ \frac{1}{B(0,0,1)}, -\frac{1-B(1,0,1)}{1+B(1,0,1)} \right\} (1 - r_0) + (1 - r_1) \end{array} \right\}. \quad (5)$$

Detailed derivations of Results 1 and 2 are in the supplementary material; we outline the general concept here.

It can be shown (see the supplementary material) that the absent arrow from U to S in Figure 1c implies the constraint,

$$A(y, 0) = A(y, 1) \text{ for all } y, \quad (6)$$

and that the absent arrow from U to S in Figure 1d implies the constraint

$$B(y, z, 0) = B(y, z, 1) \text{ for all } (y, z), \quad (7)$$

provided that sampling was not deterministic, meaning that among the cases or controls we samples randomly with probability between 0 and 1, i.e. $0 < p\{S = 1|Y = y\} < 1$, $\forall y$. Although non-deterministic sampling is required for constraints (6) and (7) to hold, the bounds derived from these constraints are valid provided that the ratios $A(y, 1)$ and $B(y, z, 1)$ are not undefined, i.e. provided that the probabilities $p_{0y.1}$ in the denominators of $A(y, 1)$ and $p_{1y1.z}$ in the denominators of $B(y, z, 1)$ are not zero; detail provided below and in the supplementary material.

To derive bounds for θ in the setting of Figure 1c that take the constraint in (6) into account we proceed as follows. We partition the term $p_{01} + p_{10}$ in (1) to

$$p_{01} + p_{10} = (p_{01.1} + p_{10.1})r + (p_{01.0} + p_{10.0})(1 - r). \quad (8)$$

We show in the supplementary material that, under the constraint in (6), the unobserved part $p_{01.0} + p_{10.0}$ is bounded by

$$p_{01.0} + p_{10.0} \geq \min \left\{ \frac{1}{1 + A(1, 1)}, \frac{A(0, 1)}{1 + A(0, 1)} \right\} \quad (9)$$

and

$$p_{01.0} + p_{10.0} \leq \max \left\{ \frac{1}{1 + A(1, 1)}, \frac{A(0, 1)}{1 + A(0, 1)} \right\}. \quad (10)$$

We can then combine (9) and (10) with (1) to produce the bounds for θ . However, these bounds are only valid and informative if $A(y, 1)$ is defined; the ratio $A(y, 1)$ is undefined if $p_{0y.1} = 0$. A solution to this problem is to reverse the coding for the exposure, i.e. to define a new exposure as $x^* = 1 - x$ for which $A(y, 1)$ are inverted. Replacing x everywhere in (2) and (3) with x^* we can obtain the lower bound, l^* , and upper bound, u^* , for $\theta^* = p\{Y(x^* = 1) = 1\} - p\{Y(x^* = 0) = 1\}$. Since $\theta^* = -\theta$, these translate into bounds for θ as $-u^* \leq \theta \leq -l^*$.

This simple solution works for the bounds if the inverse ratios, $A^{-1}(y, 1)$, are not undefined. However, this may not be the case. It is possible that $p_{1y.1} = p_{0y.1} = 0$ for some y , so that both $A(y, 1)$ and $A^{-1}(y, 1)$, are undefined. For such scenarios, we suggest using the bounds in (11), for confounded sampling.

We now turn to Figure 1d. Arguing as we did for Figure 1c (see the supplementary material for details) from the random sampling IV bounds of Balke and Pearl [1997] and combining with (7) we arrive at valid bounds for θ in the setting of Figure 1d. These bounds are given in (4) and (5). Just as above, when $B(y, z, 1)$ is undefined for any y, z pair, we can instead bound $-\theta$ by defining exposure as $x^* = 1 - x$, provided that $B^{-1}(y, z, 1)$ is not undefined. When $B^{-1}(y, z, 1)$ and $B(y, z, 1)$ are both undefined for a given y and all z , then we suggest using the bounds given in (12) and (13), for confounded sampling in addition to any remaining defined terms from (4) and (5).

3.2 Confounded outcome-dependent sampling

Confounded outcome-dependent sampling is illustrated in Figures 1e and 1f, without and with an available IV, respectively. Under Figure 1e the observed data distribution is given by $p\{X, Y|S = 1\}$. If we know $p\{S = 1\}$, the joint probabilities $p\{X = x, Y = y, S = 1\} = p\{X = x, Y = y|S = 1\}p\{S = 1\}$ are identifiable. Under Figure 1f the observed data distribution is given by $p\{Z, X, Y|S = 1\}$. If we observe $p\{S = 1\}$ and $p\{Z = 1\}$ and therefore, $p\{S = 1|Z\}$, the probabilities

$$p\{X = x, Y = y, S = 1|Z = z\} = \frac{p\{Z = z, X = x, Y = y|S = 1\}}{\sum_{x,y} p\{Z = z, X = x, Y = y|S = 1\}} p\{S = 1|Z = z\}$$

are identifiable. This holds, respectively, for Figures 1g-1h, as well.

Result 3: The bounds for θ given in (11) are valid and tight in the setting of Figure 1e, and the bounds given in (12) and (13) are valid and tight in the settings of Figure 1f, provided that $p_{xy1} \forall x, y$ (for Figure 1e) or that $p_{xy1.z} \forall x, y, z$ (for Figure 1f) are known.

$$p_{111} + p_{001} - 1 \leq \theta \leq 1 - p_{011} - p_{101}. \quad (11)$$

For Figure 1f the resulting bounds are,

$$\theta \geq \max \left\{ \begin{array}{l} p_{001.1} - p_{011.0} - p_{111.0} + 2p_{111.1} - 1 \\ p_{001.1} + p_{111.0} - 1 \\ p_{001.0} + p_{111.1} - 1 \\ p_{001.1} + p_{111.1} - 1 \\ p_{001.0} - p_{011.1} + 2p_{111.0} - p_{111.1} - 1 \\ -p_{001.0} + 2p_{001.1} - p_{101.0} + p_{111.1} - 1 \\ p_{001.0} + p_{111.0} - 1 \\ 2p_{001.0} - p_{001.1} - p_{101.1} + p_{111.0} - 1 \\ 2p_{001.0} - p_{001.1} - p_{101.1} - p_{011.1} + 2p_{111.0} - p_{111.1} - 1 \\ -p_{001.0} + 2p_{001.1} - p_{101.0} - p_{011.0} - p_{111.0} + 2p_{111.1} - 1 \end{array} \right\}, \quad (12)$$

and

$$\theta \leq \min \left\{ \begin{array}{l} -p_{101.0} - 2p_{011.0} + p_{011.1} + p_{111.1} + 1 \\ -p_{101.1} + p_{011.0} - 2p_{011.1} + p_{111.0} + 1 \\ p_{001.1} - 2p_{101.0} + p_{101.1} - p_{011.0} + 1 \\ -p_{101.0} - p_{011.1} + 1 \\ -p_{101.1} - p_{011.0} + 1 \\ -p_{101.0} - p_{011.0} + 1 \\ p_{001.1} - 2p_{101.0} + p_{101.1} - 2p_{011.0} + p_{011.1} + p_{111.1} + 1 \\ -p_{101.1} - p_{011.1} + 1 \\ p_{001.0} + p_{101.0} - 2p_{101.1} - p_{011.1} + 1 \\ p_{001.0} + p_{101.0} - 2p_{101.1} + p_{011.0} - 2p_{011.1} + p_{111.0} + 1 \end{array} \right\}. \quad (13)$$

To prove Result 3, we show (see the supplementary material), that given the probabilities p_{xy1} (for Figure 1e) or $p_{xy1.z}$ (for Figure 1f), the problem of bounding θ can be expressed as a linear programming problem. Solving the linear programming problems yields the bounds in equations (11), and (12) and (13).

3.3 Confounded exposure- and outcome-dependent sampling

Confounded exposure- and outcome-dependent sampling is illustrated in Figures 1g and 1h, without and with an available IV, respectively.

Result 4: The bounds for θ given in (11), and in (14) and (15) are valid and tight in the settings of Figure 1g and Figure 1h, respectively, provided that $p_{xy1} \forall x, y$ (for Figure 1g) or

$p_{xy1.z} \forall x, y, z$ (for Figure 1h) are known.

$$\theta \geq \max \left\{ \begin{array}{l} p_{001.1} + p_{111.1} - 1 \\ p_{001.0} + p_{111.1} - 1 \\ p_{001.1} + p_{111.0} - 1 \\ p_{001.0} + p_{111.0} - 1 \\ 2p_{001.1} + p_{011.0} + p_{111.0} + p_{111.1} - 2 \\ 2p_{001.0} + p_{011.1} + p_{111.0} + p_{111.1} - 2 \\ p_{001.0} + p_{001.1} + p_{101.0} + 2p_{111.1} - 2 \\ p_{001.0} + p_{001.1} + p_{101.1} + 2p_{111.0} - 2 \end{array} \right\}, \quad (14)$$

and

$$\theta \leq \min \left\{ \begin{array}{l} -p_{101.0} - p_{011.0} + 1 \\ -p_{101.1} - p_{011.0} + 1 \\ -p_{101.0} - p_{011.1} + 1 \\ -p_{101.1} - p_{011.1} + 1 \\ -p_{001.0} - p_{101.0} - p_{101.1} - 2p_{011.1} + 2 \\ -p_{001.1} - p_{101.0} - p_{101.1} - 2p_{011.0} + 2 \\ -2p_{101.0} - p_{011.0} - p_{011.1} - p_{111.1} + 2 \\ -2p_{101.1} - p_{011.0} - p_{011.1} - p_{111.0} + 2 \end{array} \right\}. \quad (15)$$

Just as above, it can be shown that, given the probabilities p_{xy1} (for Figure 1g) or $p_{xy1.z}$ (for

Figure 1h) are known, the problem of bounding θ can be expressed as a linear programming problem. Solving the linear programming problem yields the bounds in (14) and (15). For the setting of Figure 1g the resulting bounds are the same as for Figure 1h given in (11).

3.4 Comparison and refinement of the bounds

One would expect that the bounds in (2) and (3) (corresponding to Figure 1c) are at least as wide as the bounds in (1), and that the bounds in (11) (corresponding to Figure 1e) are at least as wide as the bounds in (2) and (3). Using the relations in (8), (9) and (10), it can easily be shown that this is indeed the case.

However, a similar relation does not hold for the bounds corresponding to Figures 1d and 1f. One can generate probabilities $p_{zxy,1}$ which are possible in the setting of Figures 1d (see supplementary material for specific scenario) where the bounds given by (12), (13) are narrower than those given by (4), (5).

An important implication of the existence of such a scenario is that the bounds in (4) and (5) are not tight. This is because, if they were, they would never be wider than any other bounds for θ in the setting of Figure 1d based on the same information. In particular, they would never be wider than the bounds in (12) and (13), since we assume the same available information and the causal diagram in Figure 1d is a special case of the causal diagram in Figure 1f, which implies that the bounds in (12) and (13) are also valid for Figure 1d.

This argument, however, suggests a simple way to improve the bounds in (4) and (5), namely to replace them with the bounds in (12) and (13) whenever these are tighter. Formally, let l_d and u_d be the lower and upper bounds in (4) and (5), and let l_f and u_f be the

lower and upper bounds in (12) and (13). We thus define new bounds for θ under the causal diagram in Figure 1d as

$$\max(l_d, l_f) \leq \theta \leq \min(u_d, u_f). \quad (16)$$

We use these bounds for Figure 1f in the remainder of the paper.

4 Simulation

To compare the derived bounds we carried out a simulation study. We generated probability distributions $p\{U, Z, X, Y, S\}$ under the causal diagram in Figure 1h from the model

$$\left. \begin{aligned} p\{U = 1\} &\sim \text{Unif}(0, 1) \\ p\{Z = 1\} &\sim \text{Unif}(0, 1) \\ p\{X = 1|U, Z\} &= \text{expit}(\alpha_1 + \alpha_2 U + \alpha_3 Z + \alpha_4 UZ) \\ p\{Y = 1|U, X\} &= \text{expit}(\beta_1 + \beta_2 U + \beta_3 X + \beta_4 UX) \\ p\{S = 1|U, Y\} &= \text{expit}(\gamma_1 + \gamma_2 Y + \gamma_3 U + \gamma_4 X) \\ (\alpha_1, \alpha_2, \alpha_3, \alpha_4, \beta_1, \beta_2, \beta_3, \beta_4, \gamma_1, \gamma_2) &\sim N(0, 5) \\ \gamma_3 &\sim N(0, \sigma_U^2) \\ \gamma_4 &\sim N(0, \sigma_X^2) \end{aligned} \right\} \quad (17)$$

where $\text{expit}(x) = e^x / (1 + e^x)$ and where e is Euler's number. In this model, σ_U and σ_X determine the degree of exposure dependence and confounding of the sampling; e.g. if $\sigma_U = 0$, then the sampling is unconfounded, and if $\sigma_X = 0$, then the sampling does not

depend on the exposure. We first generated 100,000 distributions $p\{U, Z, X, Y, S\}$ from the model in (17), with $\sigma_U = \sigma_X = 0$. For each distribution we computed our proposed bounds corresponding to the assumed causal diagrams in Figures 1c-1h. For comparison we also computed the previously derived bounds for random sampling, without [Robins, 1989] and with an IV [Balke and Pearl, 1997]. We emphasize that these bounds use the distributions $p\{X, Y\}$ and $p\{Z, X, Y\}$, respectively, which do not condition on $S = 1$. Thus, these bounds are not applicable when there is non-random (e.g. outcome-dependent) sampling.

Figure 2 shows the distribution of the width of the bounds. As expected, we observe that an available IV generally makes the bounds narrower (b vs a, d vs c, f vs e, h vs g), and that stronger deviation from the ideal randomized trial with random sampling generally makes the bounds wider (a vs c vs e, b vs d vs f). However, an exception from the latter is when exposure dependence is allowed for; the bounds under Figures 1g and 1e are always identical, and the bounds under Figures 1h and 1f are often very similar, although not always identical. The availability of an IV does not seem to generally ‘compensate’ for a non-ideal sampling scheme; the median width under Figure 1d (outcome-dependent unconfounded sampling, available IV) is larger than the median width under Figure 1a (random sampling, no available IV), and the median width under Figure 1f (outcome-dependent confounded sampling, available IV) is larger than the median width under Figure 1c (outcome-dependent unconfounded sampling, no available IV).

We next repeated the simulation for $\sigma_U = 0, 1, 2, \dots, 10$, holding σ_X fixed at 0 (top row of Figure 3), and for $\sigma_X = 0, 1, 2, \dots, 10$, holding σ_U fixed at 0 (bottom row of Figure 3). For each combination of (σ_U, σ_X) we computed the median width of the bounds (left column of Figure 3) and the proportion of time the bounds were violated (i.e. the proportion of times

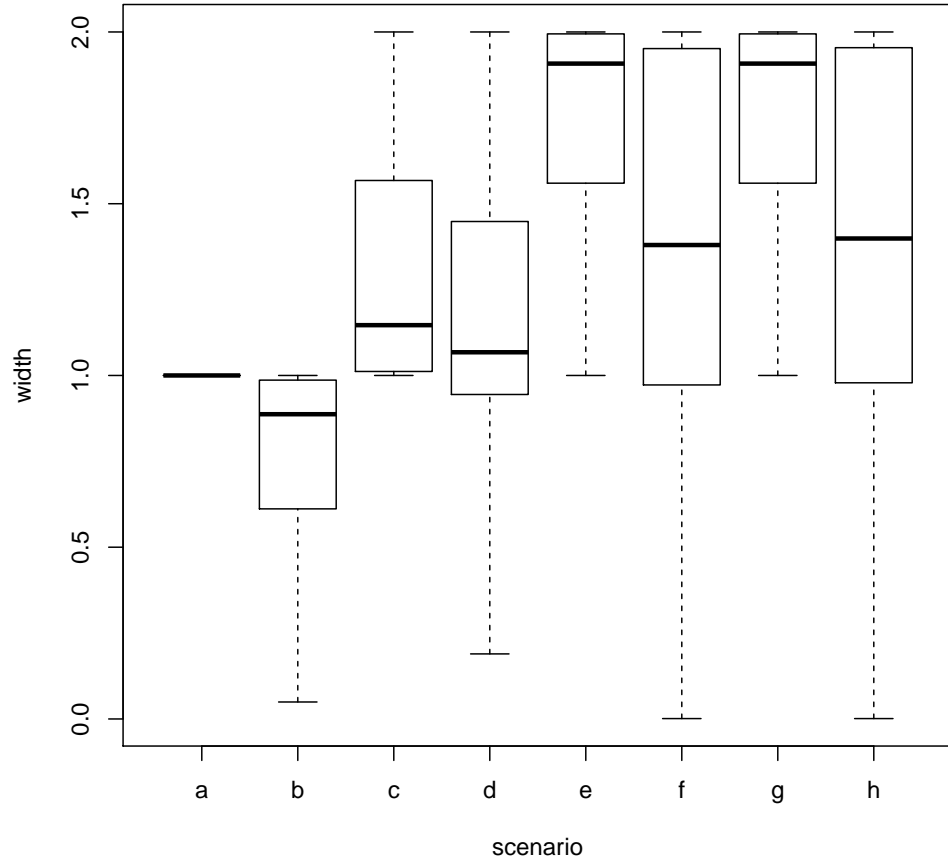


Figure 2: Width of the bounds when $\sigma_U = \sigma_X = 0$ (unconfounded outcome-dependent sampling).

the true causal risk difference is outside the bounds; right column of Figure 3). We observe that the median width is virtually constant across σ_U and σ_X for all eight bounds. When $\sigma_U > 0$, the bounds under Figures 1c and 1d are not generally valid, since these bounds assume unconfounded sampling. Thus, when $\sigma_U > 0$ we would expect that these bounds are sometimes violated. Similarly, when $\sigma_X > 0$, the bounds under Figures 1c, 1d and 1f are not generally valid, since these bounds assume sampling that is not directly dependent on the exposure. Thus, when $\sigma_X > 0$ we would expect that these bounds are sometimes violated. We observe that, although violations do indeed occur when $\sigma_U > 0$, they are very rare; at $\sigma_U = 10$ the bounds under Figures 1c and 1d are violated for less than 1% of all simulated distributions. When $\sigma_X > 0$, violations appear to be relatively common for the bounds under Figures 1d and 1f; at $\sigma_X = 10$ these bounds are violated for almost 10% of all simulated distributions. However, the bounds under Figure 1c appear to be more robust, with a the risk of violation less than 1% at $\sigma_X = 10$.

5 Real Data Example

To illustrate the performance of the bounds we use data from a real cohort study on Vitamin D and mortality, described by Martinussen et al. [2019]. To allow for public availability, the data were slightly mutilated before inclusion in the R package `ivtools`, whence we obtained the data. The exposure (X) is vitamin D level at baseline, measured as serum 25-OH-D (nmol/L). As vitamin D levels below 30 nmol/L indicate vitamin D deficiency [Martinussen et al., 2019], we used this level as a cutoff for defining a binary exposure. The outcome (Y) is death during follow-up. The data also contain an IV, a binary indicator of whether

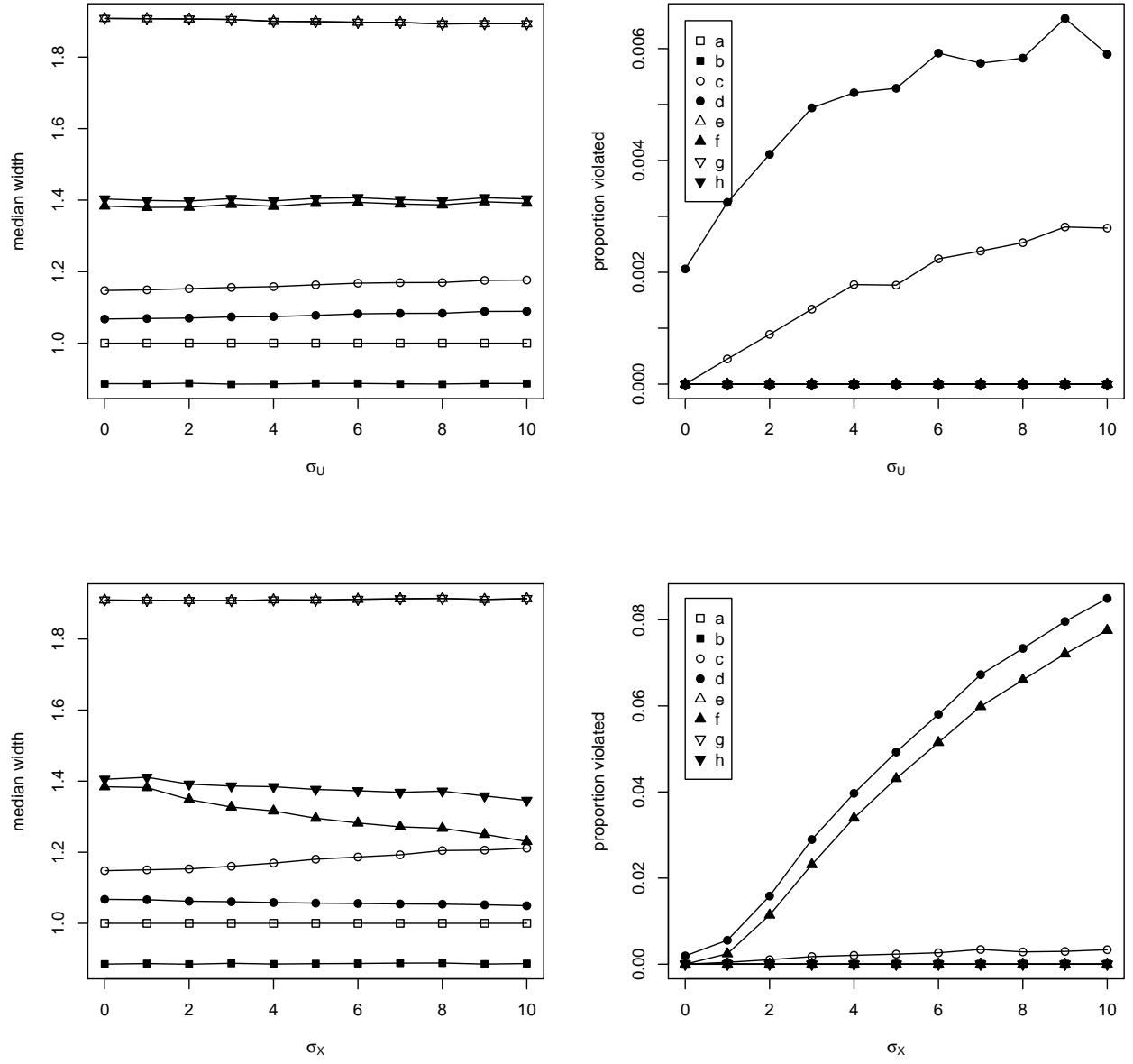


Figure 3: Median width of the bounds (left column) and proportion violated (right column), as a function of σ_U (top row) and σ_X (bottom row).

the subject has mutations in the flaggrin gene. Martinussen et al. [2019] used this IV to estimate the causal effect of vitamin D on mortality, assuming a parametric structural Cox model. In contrast, the bounds that we have derived do not make any parametric model assumptions.

The data constitute a random sample, which makes it possible to compute the bounds corresponding to Figures 1a and 1b; these are given by $(-0.74, 0.26)$ and $(-0.71, 0.15)$, respectively. Thus, for these data, the presence of an IV reduces somewhat the range of possible values for θ .

To illustrate the impact of outcome-dependent sampling, we generated a selection variable (S) randomly for each subject from a Bernoulli distribution with probability $p\{S = 1|Y = y\} = \text{expit}(\alpha + \beta y)$. Sampling is therefore dependent on the outcome, but is unconfounded and does not depend on the exposure. We set β to 0.5, to simulate sampling that is moderately outcome-dependent. We used three values of α , corresponding to the marginal selection probabilities $p\{S = 1\} = (0.1, 0.5, 0.9)$.

For each level of sampling, we computed the bounds under the assumed DAGs in Figures 1c-1h; Table 1 shows the results. As in the simulation, we observe that an available IV generally makes the bounds narrower, and that stronger deviation from the ideal randomized trial with random sampling generally makes the bounds wider. As expected, we also observe that all bounds become narrower as the probability of selection increases.

Assumed DAG	$p\{S = 1\} =$		
	0.1	0.5	0.9
c	(-0.90, 0.89)	(-0.82, 0.61)	(-0.75, 0.34)
d	(-0.90, 0.76)	(-0.81, 0.54)	(-0.74, 0.21)
e	(-0.96, 1.00)	(-0.85, 1.00)	(-0.76, 1.00)
f	(-0.96, 0.84)	(-0.81, 0.62)	(-0.74, 0.21)
g	(-0.96, 1.00)	(-0.85, 1.00)	(-0.76, 1.00)
h	(-0.96, 0.88)	(-0.84, 0.63)	(-0.76, 0.26)

Table 1: Bounds for θ under outcome-dependent sampling of the vitamin D-data.

6 Discussion

We provide valid and informative nonparametric bounds for the causal risk difference under six DAGs that cover a large number of settings for which, at least to our knowledge, the bounds had not yet been derived. This provides a nearly complete set of bounds for outcome-dependent sampling settings.

Although the Balke-Pearl method is the basis for our bounds, modifications and/or extensions to the method described in Balke [1995] were required in all settings, as none of the settings clearly define linear programming problems. In addition, our procedure requires modification of the algorithm to allow for the sampling variable $S = 1$ to define the observed data distribution, which was not considered in Balke [1995], or, to our knowledge, in subsequent literature.

As the unconfounded outcome-dependent sampling setting is not a linear optimization problem under our assumed external information, the derivation for the bounds in this setting is novel. Our approach also provides a possible route for the derivation of bounds in other settings where the constraints are nonlinear due the lack of unmeasured confounding or lack of complete observation, or both, for one or more variables.

In outcome-dependent sampling settings, the most common estimand is the odds ratio.

This is because when sampling is uncounfounded (Figure 1c and 1d), the observed odds ratio is collapsible over S and is therefore equal to the population (i.e. marginal over S) odds ratio [Didelez et al., 2010]. However, in settings with unmeasured confounding of X and Y , the observed odds ratio does not have a causal interpretation. In addition, when there is confounding of the sampling, the observed odds ratio is no longer collapsible over S and thus, not equal to the population odds ratio. Therefore, the odds ratio is not a better target than any other causal estimand for our purposes, but is, in our opinion, less interpretable than other estimands.

A setting we did not consider is uncounfounded exposure- and outcome-dependent sampling. Although this is a possible scenario, we don't see this as a likely scenario because a practitioner would have to intentionally randomly sample conditional on both the outcome and exposure. We also do not discuss scenarios where the exposure is randomized, but the sampling is outcome-dependent and/or confounded with outcome. Although this is an interesting set of problems, this is beyond the scope of this paper and an area of future research for the authors.

References

- A. Balke and J. Pearl. Bounds on treatment effects from studies with imperfect compliance. *Journal of the American Statistical Association*, 92:1171–1176, 1997.
- Alexander Balke. *Probabilistic counterfactuals: Semantics, computation, and applications*. PhD thesis, UCLA Cognitive Systems Laboratory, 1995.

- Alexander Balke and Judea Pearl. Counterfactual probabilities: Computational methods, bounds and applications. In *Proceedings of the Tenth international conference on Uncertainty in artificial intelligence*, pages 46–54. Morgan Kaufmann Publishers Inc., 1994.
- J. Bowden and S. Vansteelandt. Mendelian randomization analysis of case-control data using structural mean models. *Statistics in Medicine*, 30(6):678–694, 2011.
- M. Cai, Z. and Kuroki, J. Pearl, and J. Tian. Bounds on direct effects in the presence of confounded intermediate variables. *Biometrics*, 64(3):695–701, 2008.
- G. B. Dantzig. *Linear Programming and Extensions*. Princeton University Press, 1963.
- Vanessa Didelez, Svend Kreiner, and Niels Keiding. Graphical models for inference under outcome-dependent sampling. *Statist. Sci.*, 25(3):368–387, 2010.
- Constantine E Frangakis and Donald B Rubin. Principal stratification in causal inference. *Biometrics*, 58(1):21–29, 2002.
- M.M. Glymour, E.J. Tchetgen Tchetgen, and J.M. Robins. Credible mendelian randomization studies: approaches for evaluating the instrumental variable assumptions. *American Journal of Epidemiology*, 175(4):332–339, 2012.
- Sander Greenland. An introduction to instrumental variables for epidemiologists. *International journal of epidemiology*, 29(4):722–729, 2000.
- Miguel A Hernán and James M Robins. Instruments for causal inference: an epidemiologist’s dream? *Epidemiology*, pages 360–372, 2006.

- Torben Martinussen, Ditte Nørbo Sørensen, and Stijn Vansteelandt. Instrumental variables estimation under a structural cox model. *Biostatistics*, 20(1):65–79, 2019.
- J. Pearl. *Causality: Models, Reasoning, and Inference*. New York: Cambridge University Press, 2nd edition, 2009.
- J.M. Robins. The analysis of randomized and non-randomized aids treatment trials using a new approach to causal inference in longitudinal studies. In L. Sechrest, H. Freeman, and A. Mulley, editors, *Health service research methodology: a focus on AIDS*, pages 113–159. US Public Health Service, National Center for Health Services Research, 1989.
- D.B. Rubin. Estimating causal effects of treatments in randomized and nonrandomized studies. *Journal of Educational Psychology*, 66(5):688–701, 1974.
- A. Sjölander. Bounds on natural direct effects in the presence of confounded intermediate variables. *Statistics in Medicine*, 28(4):558–571, 2009.
- Sheena G. Sullivan and Benjamin J. Cowling. “Crude Vaccine Effectiveness” Is a Misleading Term in Test-negative Studies of Influenza Vaccine Effectiveness. *Epidemiology*, 26(5):e60, 2015.
- Sheena G. Sullivan, Shuo Feng, and Benjamin J Cowling. Potential of the test-negative design for measuring influenza vaccine effectiveness: a systematic review. *Expert Review of Vaccines*, 13(12):1571–1591, 2014.
- Sheena G. Sullivan, Eric J. Tchetgen Tchetgen, and Benjamin J. Cowling. Theoretical Basis of the Test-Negative Study Design for Assessment of Influenza Vaccine Effectiveness. *American Journal of Epidemiology*, 184(5):345–353, 2016.

J.L. Zhang and D.B. Rubin. Estimation of causal effects via principal stratification when some outcomes are truncated by “death”. *Journal of Educational and Behavioral Statistics*, 28(4):353–368, 2003.